NEUTRON STREAMING

IN

FAST CRITICAL ASSEMBLIES

David C. Wade and E. M. Gelbard

Argonne National Laboratory
Argonne, Illinois

TABLE OF CONTENTS

Neutron Streaming in Fast Critical Assemblies

(I) Introduction

The coolant volume fraction in a gas cooled fast reactor (GCFR) is 50 to 55 v/o while in a liquid metal fast breeder reactor (LMFBR) it is 40 to 45 v/o. The high volume fractions of low density helium in the GCFR or sodium vapor in a sodium-voided LMFBR give rise not only to high neutron leakage rates but to leakage which is anisotropic as a result of the polarized orientation of the coolant channels. Even in the sodium-filled LMFBR, the coolant channels provide a preferential path for diffusion.

In the fast critical assemblies in use at Argonne National Laboratory both helium and sodium-voided coolant channels are simulated by 1/4 and/or 1/2 inch air gaps in a slab type geometry. (See Figures 1 and 2) In a repeating array of such cells, the consequence of this geometry is to provide two directions (parallel to the plates along their length and parallel to the plates along their widths) having a low optical thickness and one direction (perpendicular to the plates) with a higher optical thickness. Anisotropy of neutron transport results.

Recently the impact of anisotropic diffusion in fast critical assemblies has begun to receive attention. Fisher, et. al.[1], have oriented the critical assembly platelets perpendicular to and parallel to a sodium void worth traverse direction in the 9B assembly on SNEAK. Figure 3 shows the resulting difference in worth and the calculational agreement they obtained by use of Benoist[4] anisotropic diffusion coefficients.

Zolotar, et. al.[2,3], showed that accounting for anisotropic diffusion by use of Benoist's method brought calculation into closer agreement with experiment for the results of replacing the plate geometry in ZPR-6

Assembly 7 and ZPPR-2 with a composition-matched pin geometry. The reactivity effects of the pin for plate replacements are shown in Table I. The larger streaming effect observed in ZPPR-2, relative to ZPR-6, resulted from the greater axial extent of the pin zone in ZPPR-2.

An experimental program on streaming in GCFR pin geometry criticals is underway on the PROTEUS critical facility at the Swiss Federal Institute for Reactor Research.[5] The streaming study in progress at Argonne National Laboratory is aimed at both GCFR and LMFBR cores. The goals of the Argonne program are to both measure and understand the impact of neutron streaming on the neutron balance and to develop and validate calculational techniques for modeling streaming in plate critical facilities. The program is described in the following sections.

(II) Sensitivity of Reactor Integral Parameters to Leakage

The values of the infinite multiplication constant, k_∞, for the GCFR and sodium-voided LMFBR cells shown in Figures 2 and 1 are 1.45 and 1.30 respectively; so that the corresponding leakage probabilities L, are of the order of 30 and 23%. Noting that:

$$k = k_\infty(1 - L) \tag{1}$$

$$\frac{\delta k}{k} = \frac{\delta k_\infty}{k_\infty} - \frac{\delta L}{L}\frac{L}{1-L} \tag{2}$$

it may be seen that, eg, a 5% change in leakage probability will induce large eigenvalue changes (2.0% and 1.5% in the GCFR and LMFBR respectively).

Other integral parameters are less sensitive. Table II shows[6] that for the sodium voided unit cell of Figure 1, an increase in leakage hardens the flux spectrum and softens the adjoint spectrum slightly. (The cumulative scattering source

of neutrons to the lower energies is diminished by fast neutron leakage thereby hardening the spectrum, and as shown in Table II, the probability of leakage is larger at high energies than at low energies; so an increase in leakage probability adversely affects the worth of fast neutrons relative to slower neutrons.) The corresponding changes in reaction rate ratios and kinetics parameters for the unit cell are of the order of 1% as shown in Table III. The spectral changes alone induced the changes in reactivity worth shown in the second column of Table IV. (Column 1 of Table IV shows the results for the central worth i.e. with no leakage component in the value of the worth.)

The spectral variations of integral parameters for the full core follow the pattern discussed above for the unit cell. For the RZ calculational model of the ZPR-9 GCFR Phase 1 core shown in Figure 4, Figures 5 and 6 compare the radial variations of the f^{28}/f^{49} and c^{28}/f^{49} spectral indices* when streaming is neglected or accounted for using the Benoist formalism for directionally dependent diffusion coefficients. Figure 7 shows a similar comparison for the small sample worth of Pu^{239}. These preliminary calculations, which employed ENDF/B-III data, predicted a streaming correction† to the eigenvalue of 1.9%.

(III) Experimental Studies of Streaming

Regrettably, there is currently no instrument capable of direct measurements of the anisotropy of the reactor flux in plate fast critical assemblies. As a result, measurements of neutron streaming must be made by indirect means and, as discussed above, with the exception of critical mass,

---

*f^{28} and f^{49} denote the fission rate per atom per cc for ^{238}U and ^{239}Pu respectively. c^{28} denotes the capture rate per atom per cc for ^{238}U.

†The streaming correction is defined as the change in eigenvalue produced when the homogeneous isotropic diffusion coefficients are replaced by the Benoist diffusion coefficients in the calculation.

most integral parameters are relatively insensitive to leakage.

The critical mass of the ZPR-9 GCFR Phase 1 core has been determined to be1136.0±6.0 kg fissile $^{239}Pu + ^{241}Pu + ^{235}U$. An RZ, eleven-group calculation of the critical geometry produced an eigenvalue of:

$$k = 0.9736$$

using ENDF/B-IV data. Included in the above prediction is a streaming effect of:

$$\Delta k_{streaming} = -2.1\% \, \Delta k$$

obtained by using the Benoist method for anisotropic diffusion coefficients.* For comparison, the Version IV, RZ predictions of three benchmark critical assemblies are:

	k
ZPR-6, Assem. 6A	0.9893
ZPR-6, Assem. 7	0.9844
ZPR-3, Assem. 48	0.9911

These results, at this early stage of the GCFR experimental program, suggest that the streaming effect calculated for the GCFR core may be too large.

A second more or less direct indication of neutron streaming in a plate-geometry critical assembly is an azimuthal asymmetry in reaction rates at a given Z elevation in the core. The flux can be expected to peak in the quadrants of the core roughly parallel to the streaming slots (Y direction in Figure 1) and to dip in the quadrants of the core roughly perpendicular to the streaming slots. Figure 8 shows the calculation to experiment (C/E) ratios for ^{239}Pu fission in ZPPR-4, Phase 1, the LMFBR DEMO benchmark (containing

*In the Z direction of the RZ model, Benoist's $D_{||}$ was used. In the R direction of the model, $(D_{||} + D_{\perp})/2$ was used.

sodium in the coolant slots). The calculation did not account for streaming and could be expected to underpredict the flux along the Y axis and overpredict it along the X axis. Such a trend may be discernable in the C/E pattern shown in Figure 8 -- particularly in the outer core and the blanket. Similar C/E patterns are also obtained for the ^{238}U capture and the ^{235}U fission rates. This experiment is currently being recalculated with account taken of streaming in order to test the hypothesis.

In the GCFR, where this effect is expected to be stronger, an experiment designed to study the effect is being made. Foil activation traverses will be taken along the radial 0°,-45°, and -90° rays as shown in Figure 9. Then, alternate drawers in that quadrant will be turned on their sides to form a "checkerboard" loading (see Figure 10) which eliminates streaming paths in the XY plane, and the foil traverse repeated. A variation in the activation results will be associated with neutron streaming.

The replacement of a central zone of plate unit cells with a composition-matched pin unit cell arrangement alters the streaming path geometry as well as other aspects of the neutron balance. As already discussed by Zolotar, et al[3], this change in geometry can be used to test the streaming treatment used in the calculational models.

In addition to the above experiments which are particularly aimed at the study of streaming, it is recognized that the entire neutron balance is affected (albeit insensitively) by leakage. Thus, by observing the variation of calculational to experimental discrepancies in the values of integral parameters as a function of leakage, an indication of the veracity of the modeling of streaming will be obtained. In particular, the Phase 2 configuration of the GCFR critical assembly on ZPR-9 will be obtained from the Phase 1 configuration by decreasing the void volume fraction from ∿55v/o to ∿45v/o. This variation, taken with the wealth of previous experiments on sodium-voided

LMFBR configurations, will provide a range of variation in streaming void fraction and corresponding changes in integral parameters which will be valuable in testing calculational prescriptions.

(IV) Analytical and Calculational Studies of Streaming

The goal of the program is to produce a set of modeling procedures and computer codes which will correctly treat the streaming aspects of the neutron balance within the multigroup diffusion theory framework traditionally used for criticals analysis and fast reactor design. The codes involved in the study are:

VIM: a three dimensional, continuous energy Monte Carlo code;

MC^2-II: a zero dimensional, ultra-fine group slowing down code used to generate fine-group cross section libraries;

SDX: a one dimensional, fine-group unit cell code used to produce cell-average, broad group cross sections. SDX uses the fine-group library generated by MC^2-II;

ARC: a one or two dimensional multigroup diffusion theory code used in the standard analysis of ZPR criticals. It uses the broad group cross sections produced by SDX, and has the capability of using anisotropic diffusion coefficients.

The analytical study is developing on a broad and fundamental level. The discussion of the study is organized into three sections for clarity, although the presentation does not reflect the chronological sequence.

(A) Infinite Medium Studies

A basic step in the calculational streaming study has been to verify that the calculational tools correctly predict both reaction rates and neutron transport for the simple cases of (a) an infinite, homogeneous, isotropic medium, and (b) an infinite array of heterogeneous unit cells. First, for an infinite (zero leakage) homogeneous composition characteristic of an LMFBR, the MC^2-II,

SDX, and ARC codes were shown to produce integral parameters, flux spectra, etc., in excellent agreement with the VIM Monte Carlo results. Table V shows sample results for several integral parameters. The causes of slight discrepancies in ^{238}U capture and structural capture observed in the comparison calculations were identified and understood[7,8] -- they involved the cross section representation.

The infinite, isotropic medium neutron diffusion treatment in MC^2-II was tested in the following way. The VIM code was used to produce $\overline{l^2}$, the mean-squared distance traveled by a fission neutron between birth and a fission event. It is well known that in a homogeneous medium, a Taylor series expansion of the dependence of eigenvalue on fundamental mode buckling is given by:

$$\frac{\delta k}{k} = -1/2 \; B^2\overline{l^2} + \mathcal{O}(B^4) \tag{3}$$

Thus, for a small charge, δB^2, in buckling around the zero buckling case:

$$\frac{1}{k}\frac{\delta k}{\delta B^2} = -\frac{\overline{l^2}}{2} \tag{4}$$

The MC^2-II treatment of neutron transport was tested by determining $(\delta k/\delta B^2)\big|_{B^2=0}$ from several MC^2-II calculations and comparing it to the Monte Carlo value of $\overline{l^2}/2$. In this comparison the consistent P_1 approximation was solved in MC^2-II, and agreement to within 2% was attained. Further work in progress will test the SDX leakage treatment by the same technique and will investigate the impact of using the transport approximation.

Progressing next to the heterogeneous cell case, an infinite array (zero leakage) of one dimensional heterogeneous LMFBR unit cells as shown in Figure 1 was calculated. The VIM, SDX, and ARC codes were shown to produce results in excellent agreement thereby partially validating the SDX techniques for cell homogenization. Table VI displays the agreement in integral parameters.

The mathematical foundation for the extension of Eq. 3 to the non-voided infinite cell lattice case:

$$\frac{\delta k}{k} = -1/2 \; (B_x^2\overline{l_x^2} + B_y^2\overline{l_y^2} + B_z^2\overline{l_z^2}) + \mathcal{O}(B^4) \tag{5}$$

was established by Gelbard.[9] This relation and the Monte Carlo generation of the mean square distances from birth to fission is being used to test the SDX neutron transport treatment in the case of an infinite array of non-voided unit cells.

In slab lattices containing a void slot or in a voided hexagonal lattice made of small pins spaced at a large pitch such that planar void paths exist, the values of $\overline{l^2}$ along certain coordinate axes become infinite and the Taylor expansion, Eq. 5, cannot be rigorously established. In that case, if the buckling is along the Z direction only (parallel to the void slot or pin axes) the eigenvalue is given by the solution of the equation:

$$k\, S(\vec{r}) = \int [G(\vec{\rho}' \to \vec{\rho},\ |Z' - Z|)\, S(\vec{r}') \cos B_z(Z' - Z)\, d\vec{r} \qquad (6)$$

where S is the neutron fission source density, G is the Green's function for fission, and $\vec{\rho}$ is the projection of the position vector, $\vec{r}$, on the XY plane. The use of Eq. 6 for the treatment of Z leakage in lattices was, apparently, first suggested by Kohler and Ligou.[10] In the derivation of this equation it is essential that the problem configuration be uniform in the Z direction. An efficient Monte Carlo technique for solving this equation simultaneously for a range of values of B_z has been derived[9] and is being coded.

Equation 6 can be generalized to handle diffusion normal to the axis of a subassembly, but in its generalized form, it becomes awkward to solve by Monte Carlo methods. For this reason, a more general but approximate relation has been derived for the lattice eigenvalue as a function of buckling with components perpendicular to the cell axis.[9,13] A Monte Carlo algorithm which makes use of this relation in a lattice eigenvalue computation is now being programmed.

The two Monte Carlo methods will provide rigorous solutions for the dependence of k on B^2 in the presence of streaming, against which approximate techniques will be tested.

(B) Testing of Approximate Methods for Representing Anisotropic Diffusion

While anisotropy of the neutron vector flux can be treated explicitly by S_n and Monte Carlo techniques, a prescription which fits into the multi-group diffusion theory framework used for criticals analysis and reactor design is essential. Since neutron transport is controlled by the diffusion coefficient in such methods, the use of anisotropic diffusion coefficients is natural and is being used. The ARC code has been modified to accommodate this approach.

The theory underlying several of the familiar techniques (Benoist[4], Bonalumi[11]) for approximating anisotropic neutron transport by anisotropic diffusion coefficients has been critically reviewed[12], and the Benoist method selected for further validation. In this technique the unit cell averaged diffusion coefficient in direction k is generated by the relation:

$$D_k = 1/3 \frac{\sum\sum_{ij} V_i \phi_i \lambda_j P_{ij,k}}{\sum_i V_i \phi_i} \qquad (7)$$

where V_i and ϕ_i are the volumes and fluxes in subregions i of the unit cell, λ_j is the transport mean free path in region j, and

$$P_{ij,k} = \frac{3}{V_i \lambda_j} \int_{V_j} d\vec{r} \int_{V_i} d\vec{r} \frac{e^{-\Sigma |\vec{r} - \vec{r}'|}}{4\pi |\vec{r} - \vec{r}'|^2} \Omega^2_k \qquad (8)$$

is the directional probability that source neutrons in region i suffer their first collision in region j. Here Ω_k is the direction cosine. A code, BENOIST, has been written to generate D_k using the same collision probability generating routines as used in the SDX code.

In slab lattices, the Benoist diffusion coefficient for the direction parallel to the streaming slot becomes infinite when the slot becomes a true void. The same is true in a voided hexagonal lattice of small pins spaced at a large pitch.[10] This happens because, as discussed above, the mean square displacements to fission, $\overline{l^2}$ go to infinity along certain coordinates in the presence of planar void slots.

As a consequence of the above phenomenon, the value of the Benoist diffusion coefficient for GCFR and sodium voided LMFBR core mockups on ZPR depends crucially on the amount of structural material assumed to interrupt the streaming path in the calculational model. In a plate critical the void slots are interrupted in the length (Z direction in Figure 1) only by drawer fronts and backs while in the vertical (Y) direction the drawer bottoms and matrix tubes introduce additional structural material having an optical thickness roughly ten times greater than that for the Z direction. Furthermore, the physical, three dimensional unit cell must be modeled in one dimension for the SDX code used to generate cell-average cross sections. This involves moving the structural material from the drawer ends and matrix tube top and bottom into the 1D slab regions of the SDX model so as to preserve total

atoms in the unit cell. Clearly, the use of the Benoist procedure requires careful scrutiny and validation.

An alternate technique for the generation of directional diffusion coefficients has been developed[12] which (unlike the Benoist method) accounts for higher order terms in the buckling expansion on which both methods are based. This technique takes the form of two coupled transport equations which are solved by the S_n method using a special quadrature set[6] which bunches the angular mesh around the streaming direction. It produces the anisotropic diffusion coefficients directly and therefore supplements the Monte Carlo generation of the dependence of k on B^2 (described in the previous section) in providing benchmark results against which approximate techniques can be tested.

Using both the coupled transport and the Benoist techniques, a set of one dimensional comparison calculations were made[6] on an idealization of the sodium voided LMFBR cell shown in Figure 1. Here the Σ_{tot} in the void slots was successively decreased starting at a value obtained by the one dimensional modeling procedure where steel from the cell edges is introduced into the one dimensional model -- including the void slots -- and ending at a value characteristic of the optical thickness actually "seen" by a neutron moving directly down the slot. Table VII shows the results for several energy groups having high leakage. Three diffusion coefficients are listed: (1) the volume weighted, homogeneous, isotropic D, (2) the Benoist D_Z, and (3) the Benoist D_Z corrected for higher order terms. The results show that:

(a) the homogeneous, isotropic D values are substantially too small - ∿12% at nominal Σ_{tot} and ∿14-17% at low Σ_{tot}

(b) the uncorrected Benoist D is slightly (∿2%) too large at nominal density and substantially (∿10%) too large at low density.

In another comparison[6] it was shown that the Benoist D_Z value produced by the one dimensional modeling procedure in which the steel from the cell edges is smeared into the 1D slabs is in good agreement with the Benoist D_Z produced by a more realistic two dimensional calculation in which only the drawer end material was smeared into the void column. (See Table VIII.)

Table IX compares the energy dependence of the homogeneous isotropic D with the Benoist $D_\perp$ and $D_{||}$ for the GCFR unit cell shown in Figure 2. The intra-cell flux shape for use in Eq. 7 was generated by the SDX code. Alternately, it has been found that to simply assume a flat flux, in Eq. 7 will change the value of D very little. Table X shows the D values generated using the flat flux approximation.

The one-dimensional modeling procedure used with SDX, as discussed above, involves smearing structural material from the cell edges into the slab regions of the SDX model including the void column. Does this procedure significantly affect the values of cell-average, broad group cross sections produced by SDX? This problem was studied by comparing the results of two Monte Carlo calculations: one for a true three dimensional cell and one for a one-dimensional cell modeled by the SDX procedure. The cells were made 72.5 in. long -- parallel to the plates with vacuum boundary conditions to correspond to the GCFR mockup on ZPR-9. Reflecting and/or periodic conditions were used on the other cell extremities. From the edits of plate-wise isotopic microscopic cross sections produced by the two calculations it was verified that to within the statistical uncertainty (± <0.1% over most of the important

energy range) the two unit cells produced identical cross sections. Also, comparison of the two intra-cell flux shapes in different energy bands showed close agreement. This agreement indicates that cross sections and plate self-shielding factors are not significantly affected by the approximations made in the one-dimensional modeling approach.

Also from the Monte Carlo comparison, Table XI displays the fractions of Z leakage going out each of the void and non-void columns at the end of the unit cell. In addition, the area fractions subtended by these columns are shown. The close correlation indicates that the Z leakage is almost uniformally distributed across the end of the cell and is not localized to the void columns. It is noted that the total mean-free path is of the same characteristic length as the drawer width (see Table II).

(C) Model Problem For Anisotropic Diffusion In Finite, Multimedia Configurations

The testing of the Benoist method is currently being pursued for the model problem shown in Figure 11. In this model which is an idealization of a core surrounded by a blanket, leakage is constrained to occur in the X direction only. The plates and void slots are oriented first perpendicular to and then parallel to the X axis and Monte Carlo solutions are obtained for each configuration. The ARC diffusion theory results using group constants from the SDX and BENOIST codes will be compared with the Monte Carlo standard.

In another model problem, the sodium void worth for a finite cluster of unit cells, is being computed using a new Monte Carlo perturbation technique[9]. The sodium void results obtained by standard methods are being compared to the Monte Carlo solution.

(V) Conclusion

Neutron leakage is an important component of the neutron balance in GCFR's and sodium voided LMFBR's, where the coolant volume fractions are in the range of 40-50 v/o. The leakage is anisotropic owing to the polarized orientation of the coolant channels.

The eigenvalue (or critical mass) is quite sensitive to the leakage whereas most other integral parameters are affected only slightly and indirectly through spectral shifts in the flux and adjoint. Streaming corrections $\sim 2\% \Delta k$ are calculated for the GCFR mockup on ZPR-9.

The GCFR experimental program on ZPR-9 is geared to study streaming effects through the variation of critical mass with void fraction and by examining the azimuthal asymmetry of reaction rate traverses in the presence and absence of planar streaming paths. Pin/plate comparisons are also being made.

The analytical and computational program is designed to yield a set of modeling procedures and computer codes which will correctly predict the streaming aspects of the neutron balance within the multigroup diffusion theory framework. Rigorous techniques based on Monte Carlo and S_n methods have been developed to provide benchmark results against which approximate techniques such as Benoist method can be tested. Comparison with experimental results will, of course, play an important role in the validation process.

VI Acknowledgements

The results reported here are based on the work of many staff members in the Applied Physics Division at Argonne National Laboratory. Among them are S. Bhattacharyya, C. Beck, E. Bohn, T. Daly, J. Gasidlo, H. Henryson II, P. Kier, M. Lineberry, R. McKnight, and R. Prael.

(VII) References

1. E. A. Fischer, et. al., "An Investigation of the Heterogeneity Effect in Sodium Void Reactivity Measurements," Proceedings of the International Symposium on Physics of Fast Reactors, Tokyo, Japan, October 16, 1973, Vol. 2, p. 945.

2. B. A. Zolotar, G. Grasseschi and P. H. Kier, "Analysis of Plate-Rod Heterogeneity Measurements in Demonstration Reactor Benchmark Assemblies Including the Effect of Streaming," Trans. Am. Nucl. Soc., 18, 309 (1974).

3. B. A. Zolotar, et. al., "Implications of Integral Experiment Data to LMFBR Design,: Proceedings of the ANS Topical Conference on Advanced Reactors; Physics, Design, and Economics, September 8-11, 1974, Atlanta, Ga.

4. P. Benoist, "Streaming Effects and Collision Probabilities in Lattices," Nucl. Sci. Eng., 34 285-307, (1968).

5. S. Seth, et. al., "GCFR Benchmarks; Experiments and Analysis," Conf. on Nuclear Cross Sections and Technology, March 3-7, 1975, Washington, D.C.

6. D. C. Wade and E. M. Gelbard, "Neutron Streaming in Plate Criticals," Proceedings of the ANS Topical Conference on Advanced Reactors; Physics, Design, and Economics, September 8-11, 1974, Atlanta, Ga.

7. R. E. Prael and H. Henryson II, "A Comparison of VIM and MC^2-II -- Two Detailed Solutions of the Neutron Slowing Down Problem," Conf. on Nuclear Cross Sections and Technology, March 3-7, 1975, Washington, D.C.

8. R. E. Prael, "Cross Section Preparation for the Continuous Energy Monte Carlo Code, VIM," Conf. on Nuclear Cross Sections and Technology, March 3-7, 1975, Washington, D.C.

9. E. M. Gelbard, "Monte Carlo Computation of Leakage From a System in a Fundamental Mode," ANL-RDP-34 Reactor Development Program Progress Report (November, 1974).

10. P. Kohler and J. Ligou, "Axial Neutron Streaming in Gas Cooled Fast Reactors," Nucl. Sci. Eng. 54 357-366 (1974).

11. R. A. Bonalumi, Energ. Nucl. (Milan), 18, 395 (1971).

12. E. M. Gelbard, "Anisotropic Diffusion in ZPPR Lattices," Nucl. Sci. Eng., 54 327-340, (1974).

13. E. M. Gelbard and R. Lell, "Role of the Mean Cord Length in Lattice Reactivity Calculations", Trans. Am. Nucl. Soc. 20, June, 1975.

TABLE I. Reactivity Effect of Pin for Plate Replacement*

CORE	EXPERIMENT (Ih)	CALC. NO STREAMING (Ih)	CALC. WITH STREAMING (Ih)
ZPR-6, Assembly 7	52.3 ± 3.5	57.34	56.09
ZPPR-2	78.5 ± 7.2	113.84	93.54

* Taken from Reference 3

TABLE II. Flux, Adjoint, Leakage, and Mean Free Path Versus Energy for Sodium-Voided LMFBR Unit Cell*

Group	Energy	Critically Buckled					10% Increase in Buckling	
		Flux (%)	Adjoint (%)	Leakage (%)	Accumulated Leakage (%)	Total Mean Free Path (cm)	Flux Change (%)	Adjoint Change (%)
	MeV							
1	10.	0.31	5.214	0.67	0.67	13.26	+2.27	-1.00
2	6.06	1.24	4.432	2.35	3.02	11.52	+2.26	-1.24
3	3.68	2.99	4.428	5.49	8.50	11.16	+2.04	-1.24
4	2.23	4.17	4.083	6.93	15.44	10.11	+1.97	-1.37
5	1.35	5.29	3.621	7.21	22.65	8.28	+1.79	-1.60
	keV							
6	821.	11.73	3.526	16.51	39.16	8.55	+1.01	-1.73
7	498.	9.39	3.423	9.54	48.69	6.18	+0.86	-1.23
8	302.	12.12	3.306	11.70	60.39	5.88	+0.46	-1.03
9	183.	12.05	3.193	11.41	71.80	5.76	-0.02	-0.81
10	111.	10.01	3.068	8.00	79.80	4.86	-0.44	-0.49
11	67.4	8.51	2.919	6.36	86.17	4.56	-0.87	-0.27
12	40.9	5.95	2.797	3.74	89.90	3.81	-1.16	-0.07
13	24.8	5.80	2.743	4.61	94.51	4.83	-1.49	0.00
14	15.0	3.94	2.760	2.49	97.00	3.84	-2.00	+0.29
15	9.12	2.00	2.822	0.83	97.83	2.52	-2.20	+0.40
16	5.53	1.78	2.920	0.83	98.66	2.84	-2.42	+0.51
17	3.35	1.13	3.057	0.44	99.10	2.38	-2.56	+0.62
18	2.03	0.80	3.229	0.49	99.58	3.75	-2.89	+0.62
19	1.23	0.41	3.392	0.22	99.81	3.30	-3.16	+0.77
	eV							
20	749.	0.22	3.956	0.12	99.93	3.15	-3.60	+0.86
21	454.	0.09	4.183	0.04	99.97	2.64	-4.40	+0.91
22	275.	0.07	4.582	----	----	2.95	-3.03	+0.98
23	101.	0.01	6.245	----	----	3.00	-12.50	+1.06
24	37.3	----	2.539	----	----	5.93	-----	+1.01
25	13.7	----	5.152	----	----	2.72	-----	+1.09
26	5.04	----	3.011	----	----	3.15	-----	+1.00
27	1.86	----	5.401	----	----	2.19	-----	+1.20

* Taken from Reference 6.

TABLE III. Changes in Integral Parameters Induced by a 10% Increase in Leakage

PARAMETER	VALUE AT CRITICAL	CHANGE INDUCED BY 10% INCREASE IN B^2
k	1.000	-2.54% Δk
Λ	3.956-7 sec^{-1}	-0.3%
β_{eff}	3.283-3	+0.8%
f^{28}/f^{49}	0.02578	+2.1%
f^{25}/f^{49}	1.0408	-0.5%
c^{28}/f^{49}	0.1442	-0.9%

TABLE IV. Changes in Material Worth Induced by a 10% Increase in Leakage in a Critical, Sodium Voided Unit Cell

Isotope	% Increase in Algebraic Value of Worth Due to a 10% Increase in B^2		
	(Central Worth Scattering, Capture, and Fission)	Central Worth + B^2 δ D	Central Worth + B^2 δ D + D δ B^2
^{239}Pu	3.41	3.35	3.57
^{238}U	2.78	4.99	12.07
Na	4.74	6.98	31.14
^{16}O	5.03	25.61	84.35
Fe	0.19	6.90	91.22

TABLE V. ZPR-6, Assembly 7 Homogeneous Zero Leakage Unit Cell; VIM/MC^2-II/SDX Comparison of Integral Parameters

Parameter	VIM	MC^2-II	Difference*	SDX	Difference*
k	1.2128 ± 0.0014	1.2121	-0.0007 Δk	1.2121	-0.0007 Δk
$1 + \alpha^{49}$	1.3223 ± 0.04%	1.3232	+0.068%	1.3204	-0.144%
c^{28}/f^{49}	0.1690 ± 0.15%	0.1675	-0.888%	0.1673	-1.006%
$c^{28}/(f^{49}(1 + \alpha^{49}))$	0.1278 ± 0.155%	0.1266	-0.939%	0.1267	-0.861%
f^{28}/f^{49}	0.01885 ± 0.82%	0.01862	-1.220%	0.01892	+0.371%

*Difference is computed relative to VIM.

TABLE VI. Comparison of VIM, SDX, and ARC Integral Parameters for the Heterogeneous ZPR-6, Assembly 7 Cell

Item	VIM	SDX		ARC	
		Value	Difference	Value	Difference
k	1.23961 ± 0.00165	1.24013	+0.00052	1.24029	+0.00068
$(1 + \alpha^{49})$	1.3074 ± 0.287%	1.3073	-0.008%	1.3073	-0.008%
f^{28}/f^{49}	0.01921 ± 0.985%	0.01906	-0.781%	0.01906	-0.781%
c^{28}/f^{49}	0.1664 ± 0.316%	0.1640	-1.442%	0.1640	-1.442%
σ_c^{28}	0.32032 ± 0.316%	-	-	0.31679	-1.102%
σ_f^{49}	1.9244 ± 0.218%	-	-	1.9275	+0.163%

TABLE VII. Sodium-Void Unit Cell (B^2 = 0.000576). Cell-Average Diffusion Constant Versus "Smeared" Iron Concentration in Void Channel.*

Energy Group	Density of "Smeared" Fe in Na-Void Channel (g/cc)	Anisotropic D Corrected for Higher-Order Terms	% Error in D	
			Homogeneous[a]	Benoist D_z
Group 1 6.065-10.0MeV	0.5248	4.079	-1.2	+2.8
	0.2624	4.277	-1.5	+3.5
	0.1312	4.382	-1.7	+4.0
	0.0656	4.435	-1.7	+4.4
Group 6 497.9-820.9 keV	0.5248	2.751	-6.5	+2.6
	0.2624	2.864	-7.3	+4.5
	0.1312	2.928	-7.6	+7.1
	0.0656	2.951	-7.7	+8.8
Group 9 111.1-183.2 keV	0.5248	1.964	-11.0	+2.0
	0.2624	2.008	-12.9	+4.5
	0.1312	2.117	-13.6	+7.8
	0.0656	2.135	-13.6	+10.7
Group 11 40.9-67.4 keV	0.5248	1.598	-12.8	+1.2
	0.2624	1.704	-15.2	+3.8
	0.1312	1.775	-17.1	+6.5
	0.0656	1.800	-17.5	+10.1

[a]Obtained from cell, volume-weighted Σ_{tr}.

*Taken from Reference 6.

TABLE VIII. Comparison of Benoist D's from Two-Dimensional and One-Dimensional Models*

Energy Group	2-D Model		1-D Model			Homogeneous	
	Σ_{tot} in Void Slot	Benoist D	Σ_{tot} in Void Slot	Benoist D	% Error	D	% Error
Group 6 497.9-820.9 keV	0.0013981	2.929	0.0188900	2.884	-1.54	2.710	-7.48
Group 9 111.1-183.2 keV	0.0019224	2.085	0.025960	2.032	-2.54	1.821	-12.66

*Taken from Reference 6.

TABLE IX. Directional Diffusion Coefficients for ZPR-GCFR Phase I Core Composition

Group No.	E_{Top}	$D_{Homogeneous}$[a]	D_x	D_y	$D_{Average}$[b]
1	10 MeV	4.6957	4.7048	4.9698	4.8815
2	3.678	4.0378	4.0494	4.3379	4.2417
3	1.353	3.3596	3.3749	3.7100	3.5983
4	0.498	2.3231	2.3453	2.6929	2.5770
5	0.133	2.0744	2.1003	2.4350	2.3234
6	67.3 keV	1.6531	1.6808	1.9577	1.8654
7	24.73	1.7533	1.7797	2.0666	1.9709
8	9.10	1.0258	1.0501	1.2106	1.1571
9	3.35	1.1483	1.1772	1.3740	1.3084
10	0.454	0.9727	1.0082	1.1963	1.336
11	0.4 eV	0.4872	0.7684	1.1885	1.0485

[a] $D_{Homogeneous}$: Isotropic diffusion coefficient used in normal diffusion theory calculations.

[b] $D_{Average}$: $[2/3 \cdot D_y + 1/3 \cdot D_x]$.

TABLE X. Directional Diffusion Coefficients for ZPR-GCFR Phase I Core Using a Flat Flux Assumption[a]

Group No.	E_{Top}	$D_{Homogeneous}$	D_x	D_y	$D_{Average}$
1	10 MeV	4.6957	4.7056	4.9845	4.8915
2	3.678	4.0378	4.0497	4.2456	4.2456
3	1.353	3.3596	3.3749	3.7107	3.5988
4	0.497	2.3231	2.3453	2.6927	2.5769
5	0.133	2.0744	2.1002	2.4344	2.3230
6	67.3 KeV	1.6531	1.6807	1.9571	1.8650
7	24.73	1.7533	1.7796	2.0658	1.9704
8	9.10	1.0258	1.0497	1.2089	1.1558
9	3.35	1.1483	1.1765	1.3704	1.3057
10	0.454	0.97265	1.0063	1.1885	1.1277
11	0.4 eV	0.48717	0.73533	1.1134	0.98738

[a]The ϕ_i in Eq. 7 were taken to be 1.0 everywhere.

TABLE XI. Axial Leakage Fraction Versus Area Fraction

	Cell		1-D Cell	
	Leakage Fraction (%)	Area Fraction (%)	Leakage Fraction (%)	Area Fraction (%)
Left Void Column	21.19 ± 2.4%	20.74	22.41	21.23
Right Two Void Columns	31.85 ± 2.2%	30.95	34.52	32.35
Horizontal Air Cooling Gap	2.82 ± 6.8%	3.04	-----	-----
Rest of Cell	44.13 ± 2.0%	45.36	43.05	46.42

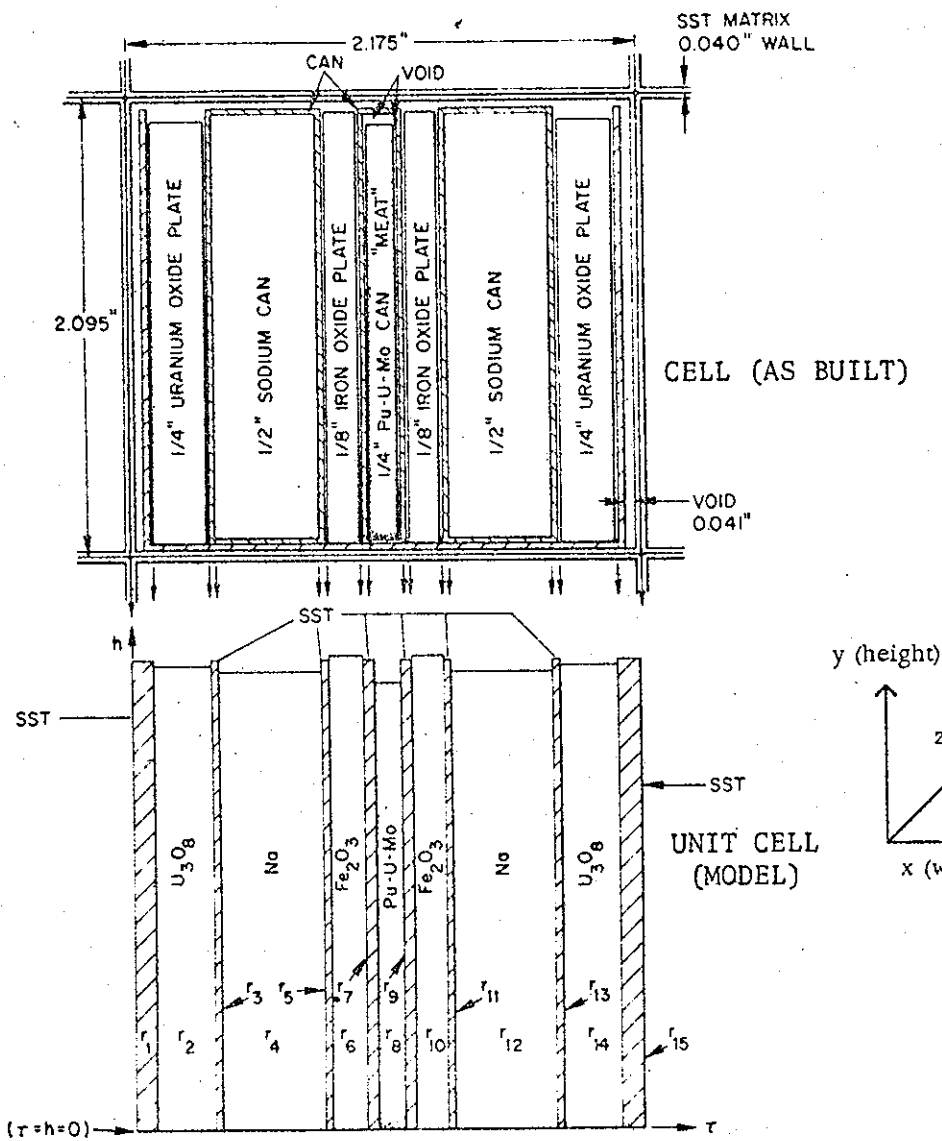

Fig. 1. LMFBR unit cell (dimensions in inches).

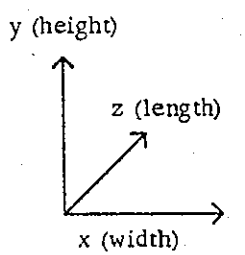

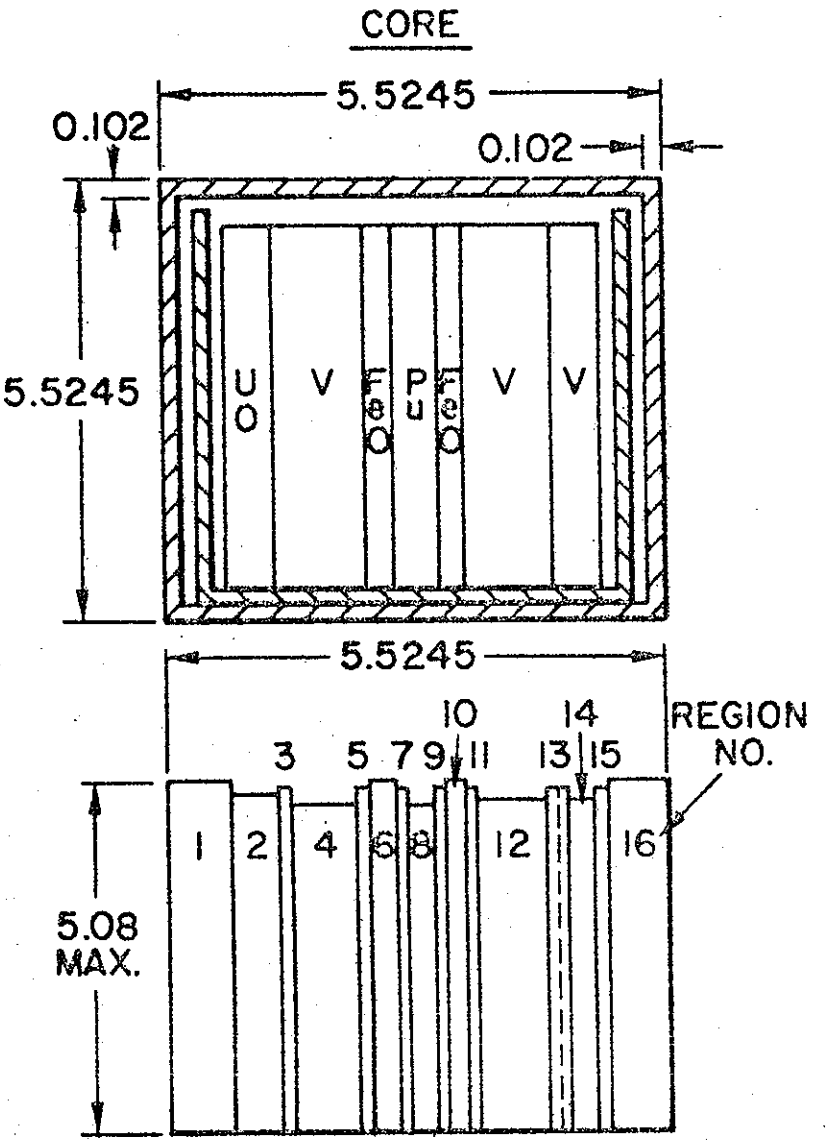

Fig. 2. GCFR unit cell (dimensions in cm).

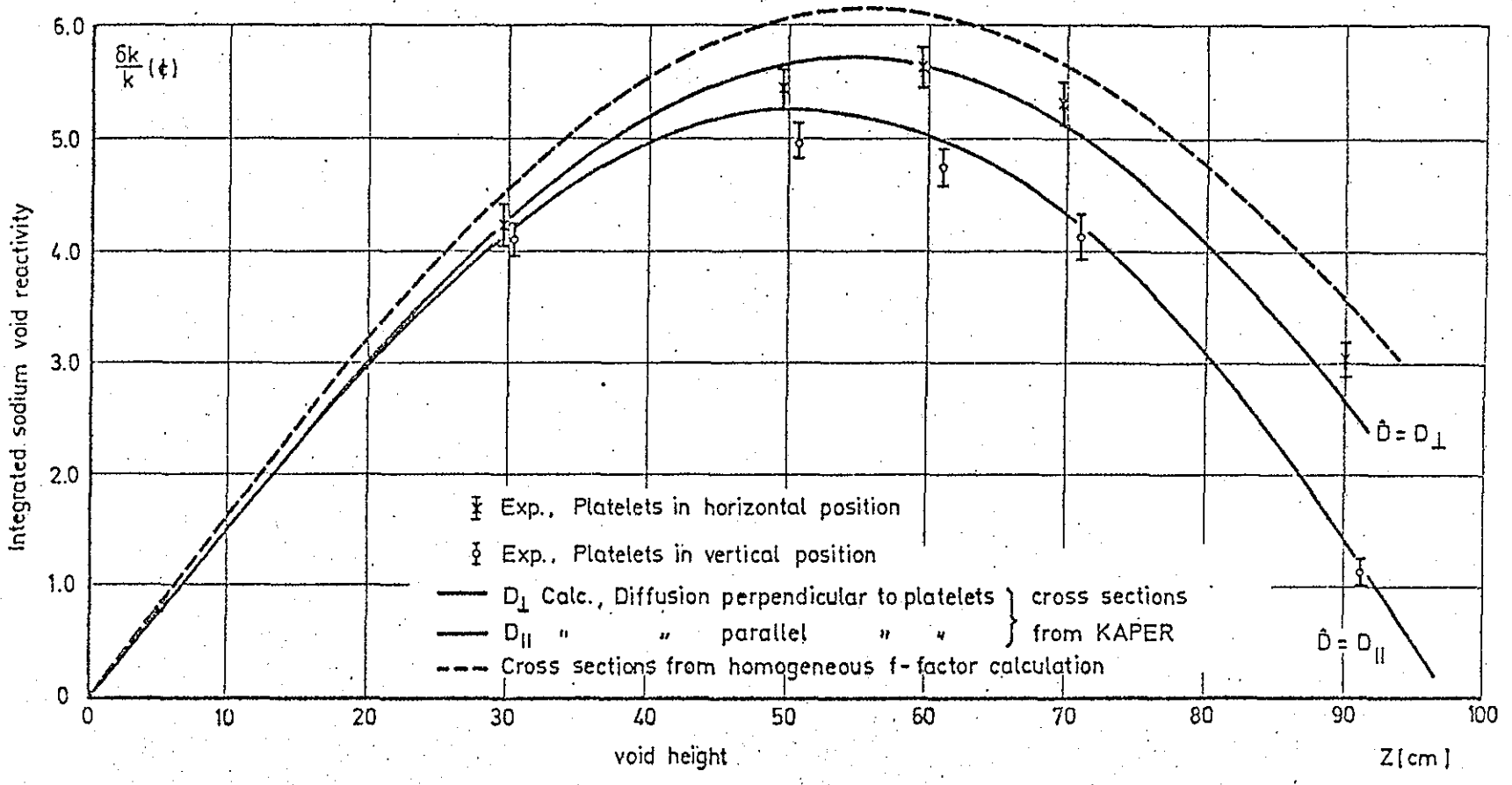

Fig. 3 Integrated axial sodium void reactivity effect, SNEAK-9B (Ref. 1).

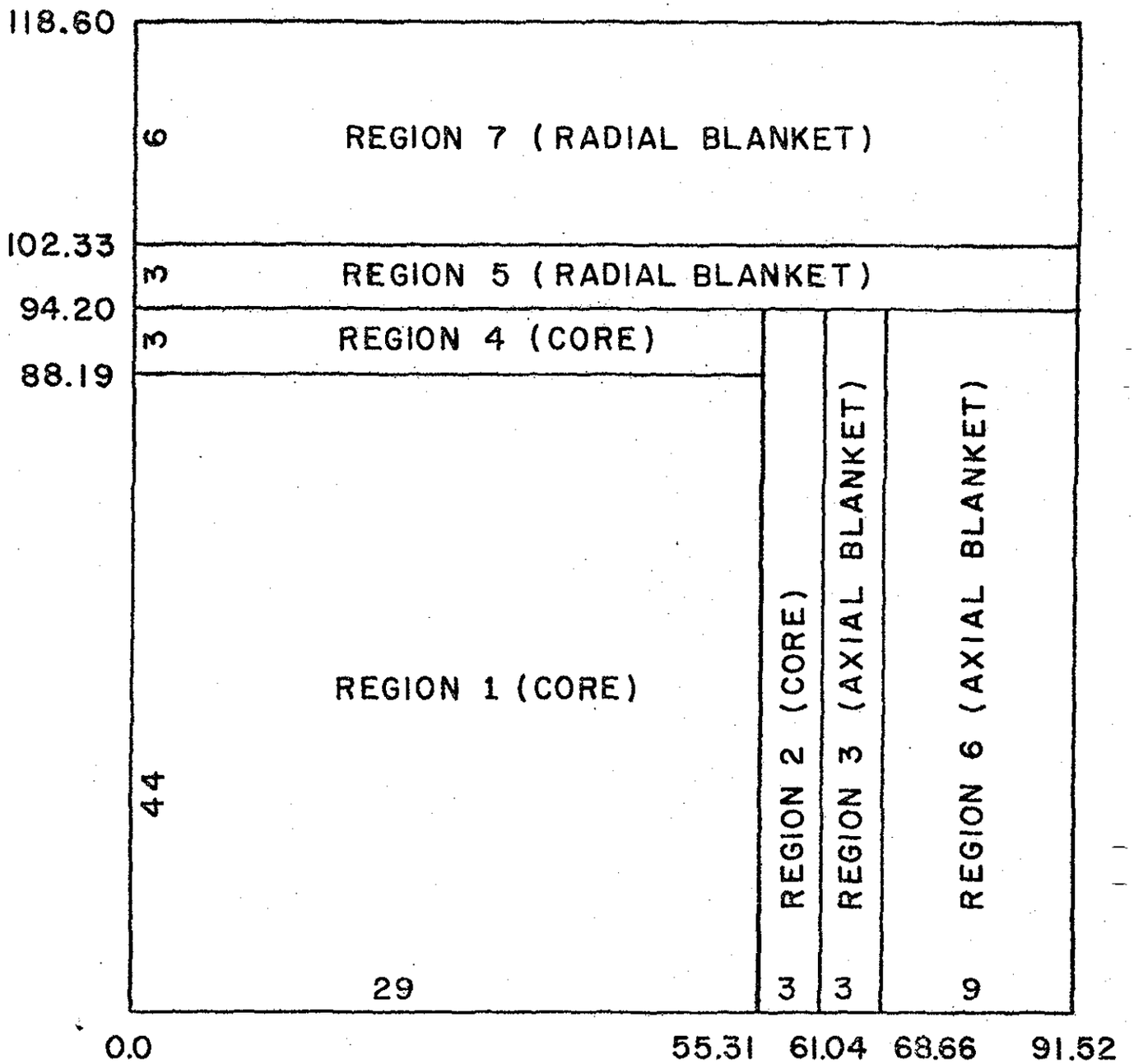

Fig. 4. R-Z Calculation Model for ZPR-GCFR Phase I Assembly. The numbers outside the drawing give the dimensions of the various regions. The numbers within the drawing give the number of mesh points used in the calculation.

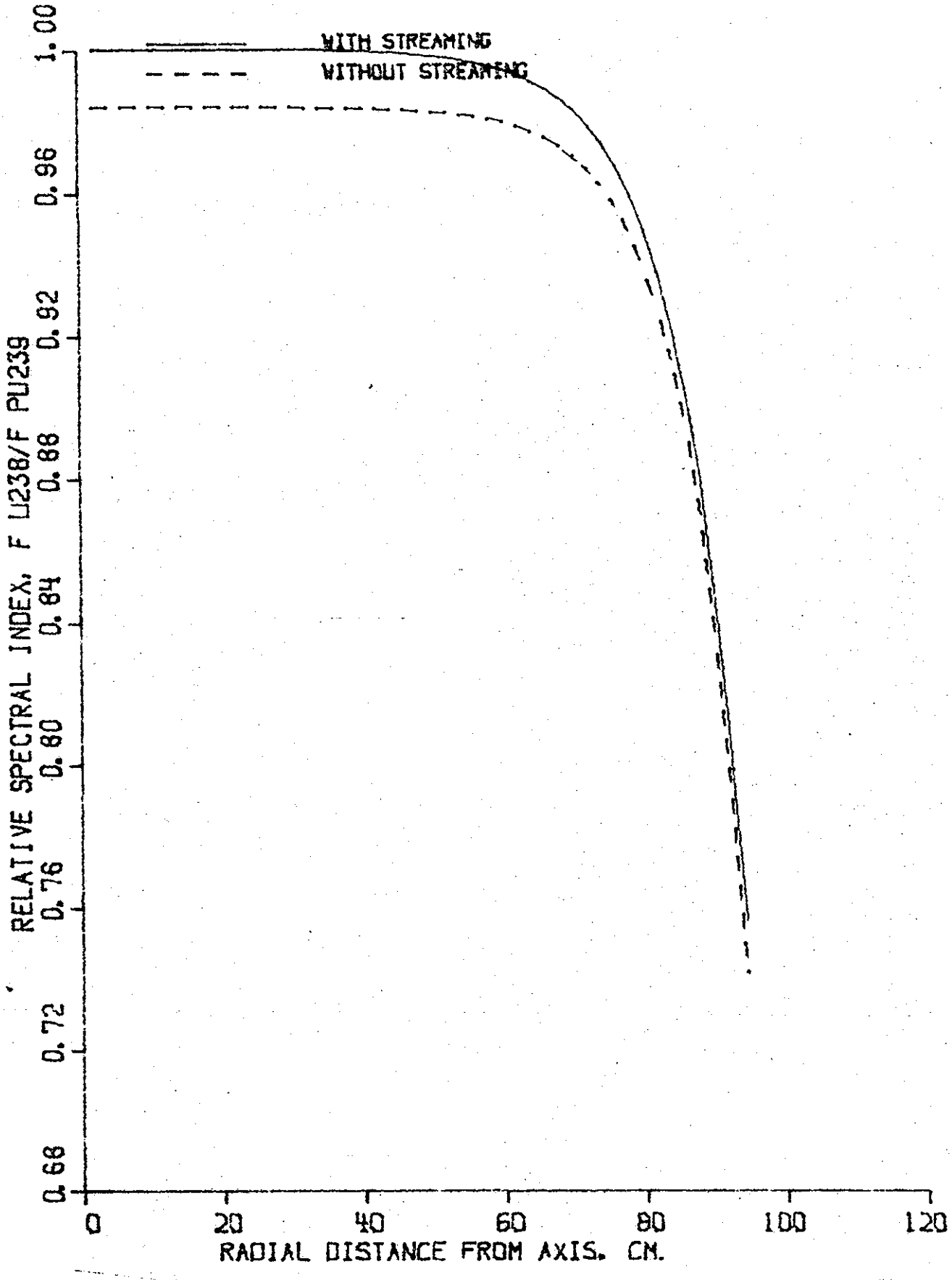

Fig. 5. Radial Variation of the Spectral Index, Fissions in U238/Fissions in Pu239. The spectral indices are relative to the Central Value.

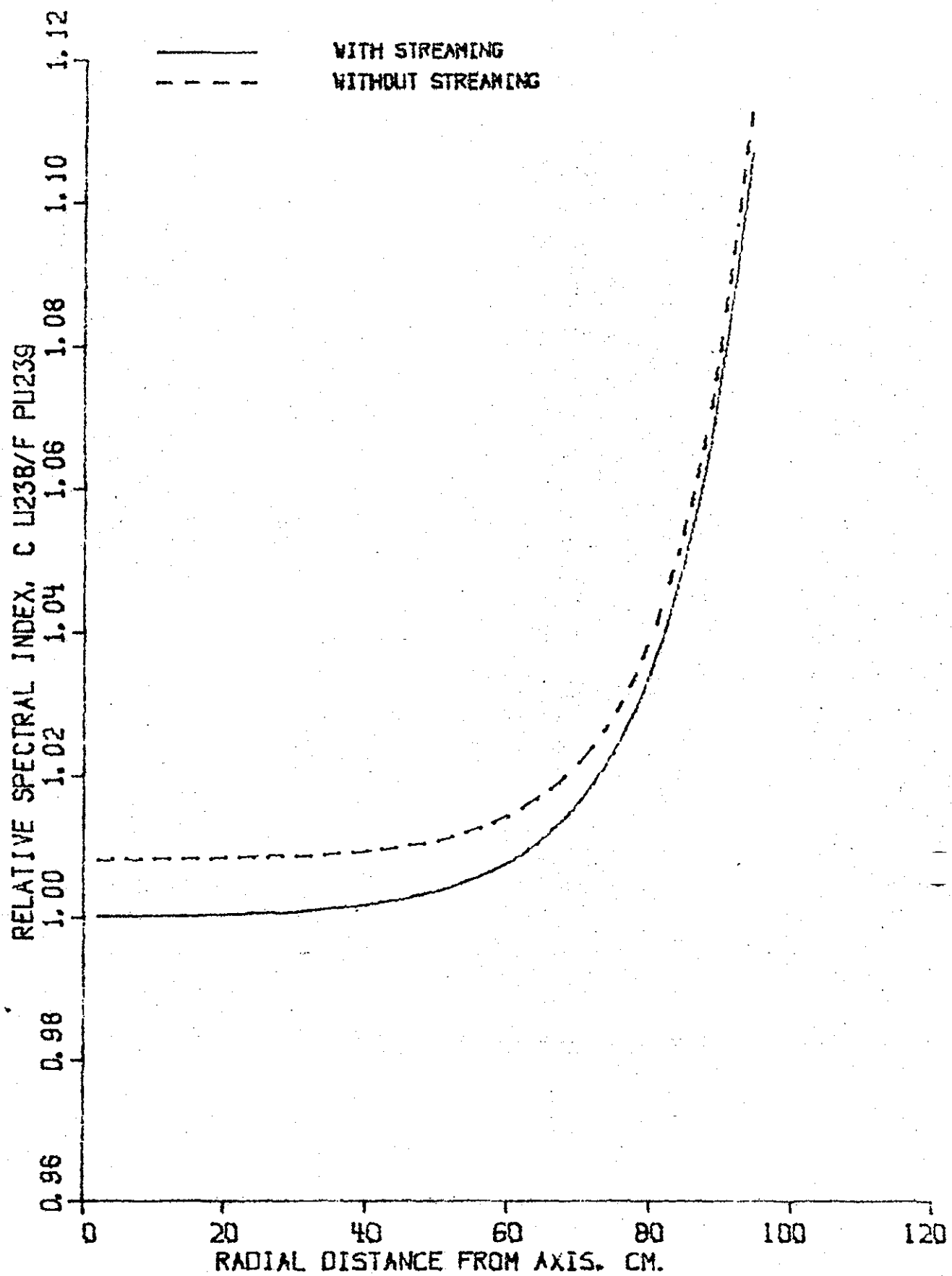

Fig. 6. Radial Variation of the Spectral Index, Captures in U238/Fissions in Pu239. The Spectral Indices are Relative to the Central Value.

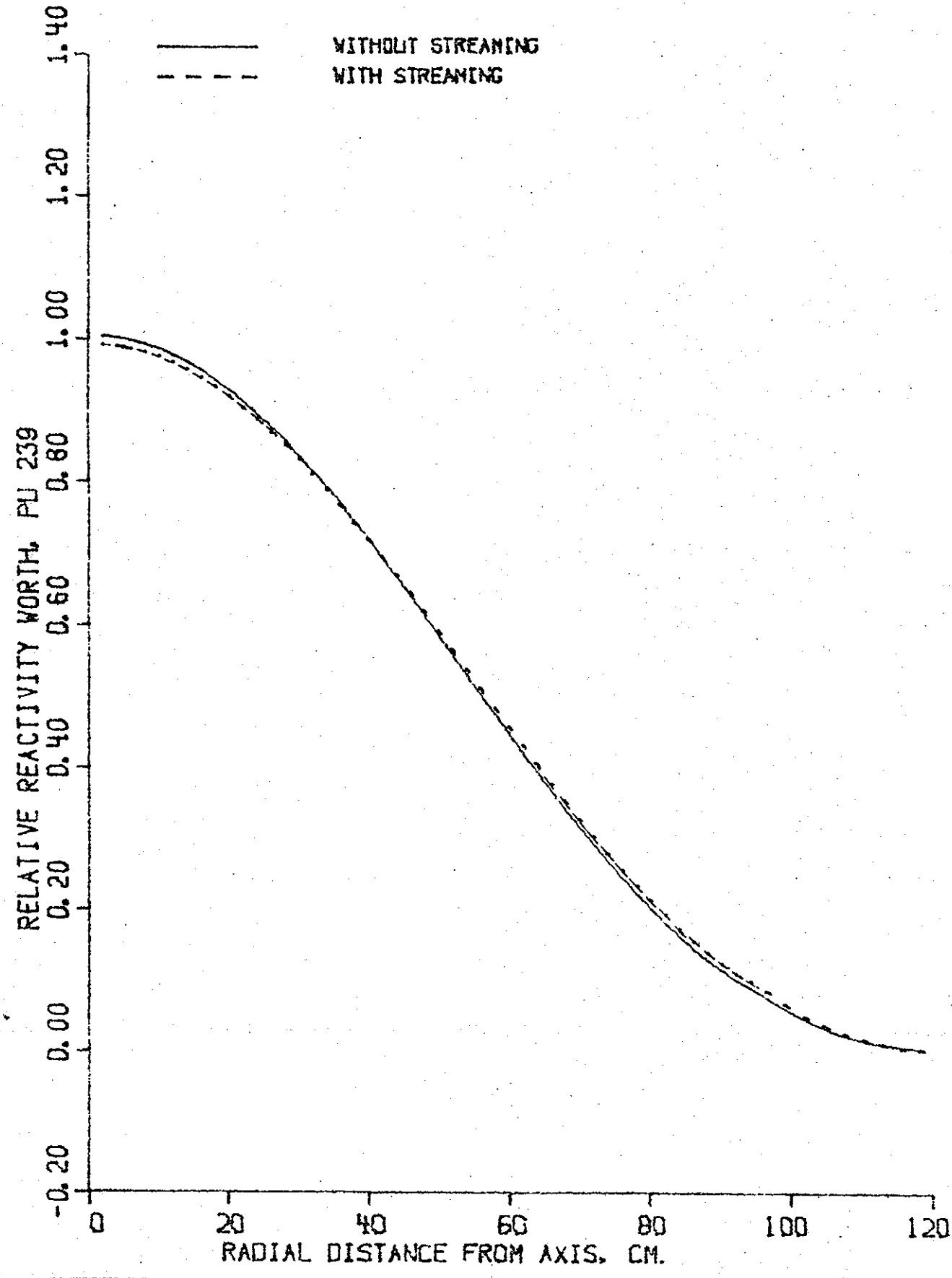

Fig. 7. Radial Variation of the Reactivity Worth of PU 239. The worths are relative to the central worth.

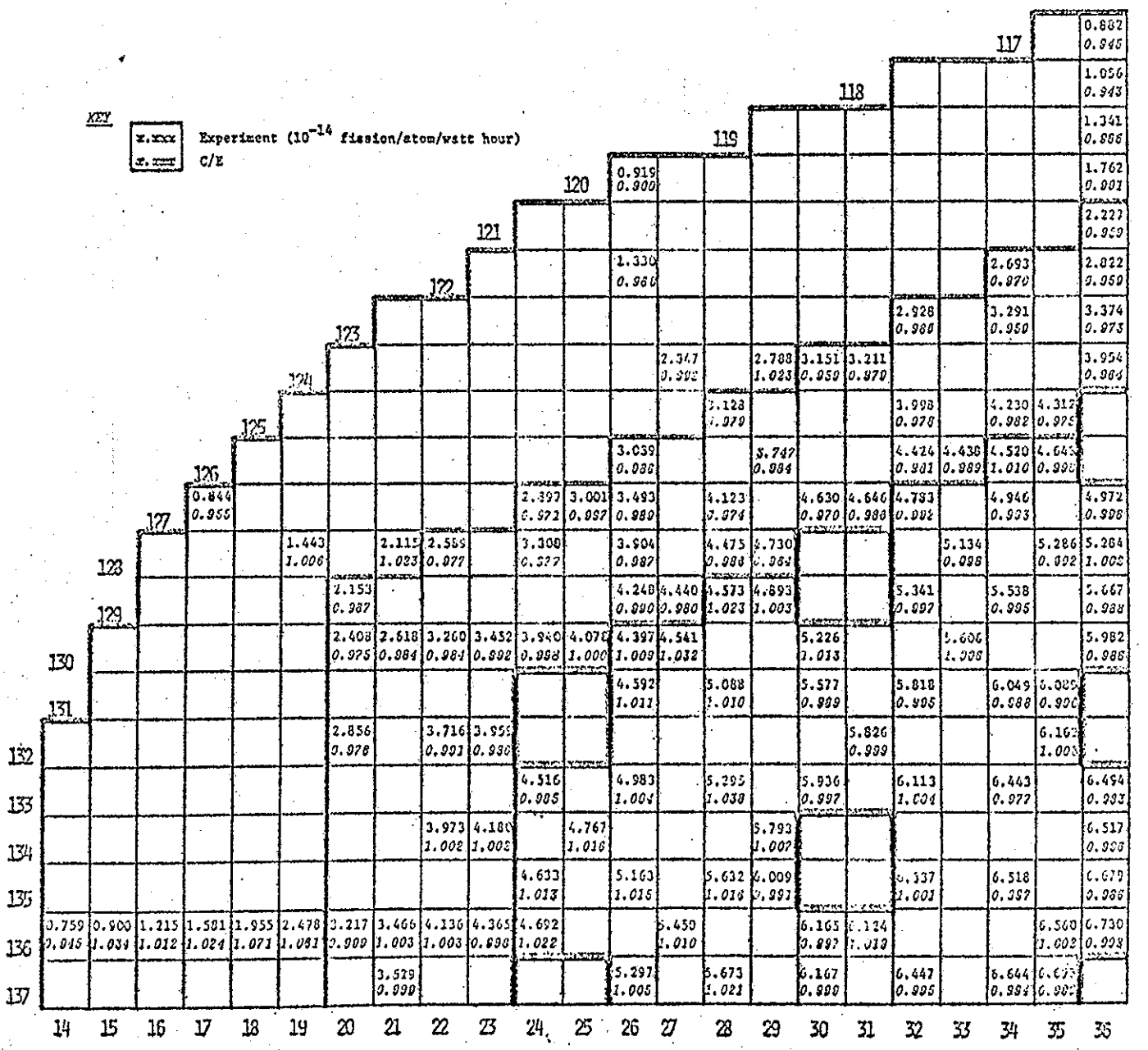

Fig. 8 ^{239}Pu(n,f) Reaction Rate Comparison ε z = 9.085 cm

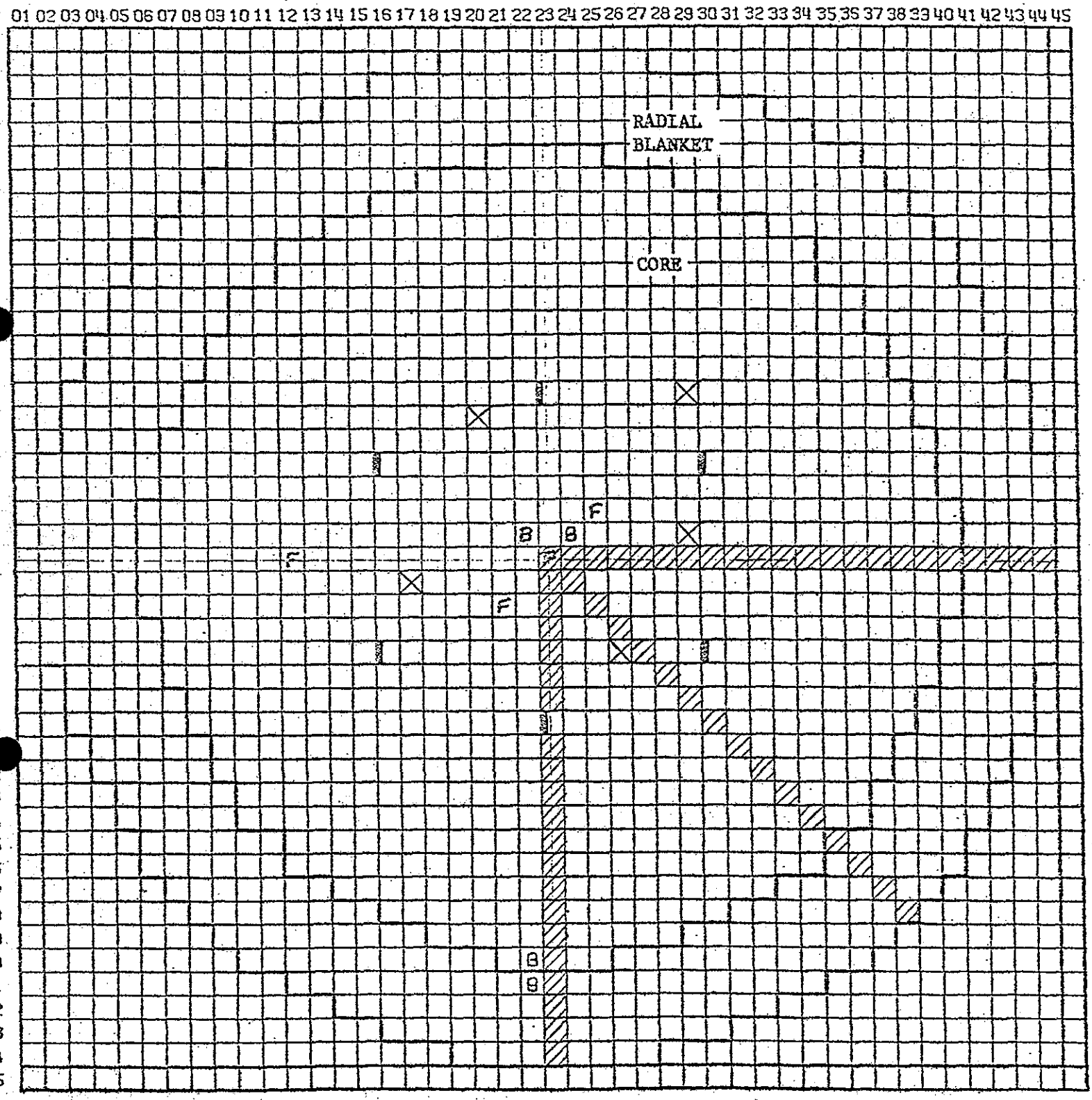

⊠ D.P. Control Rod
▯ B-10 Safety Rod
▨ Traverse Foils
Ⓕ Fission Chamber
Ⓑ Unit Cells

Fig. 9. Fission chamber, foil and unit cell measurement locations in the stationary half of ZPR-9.

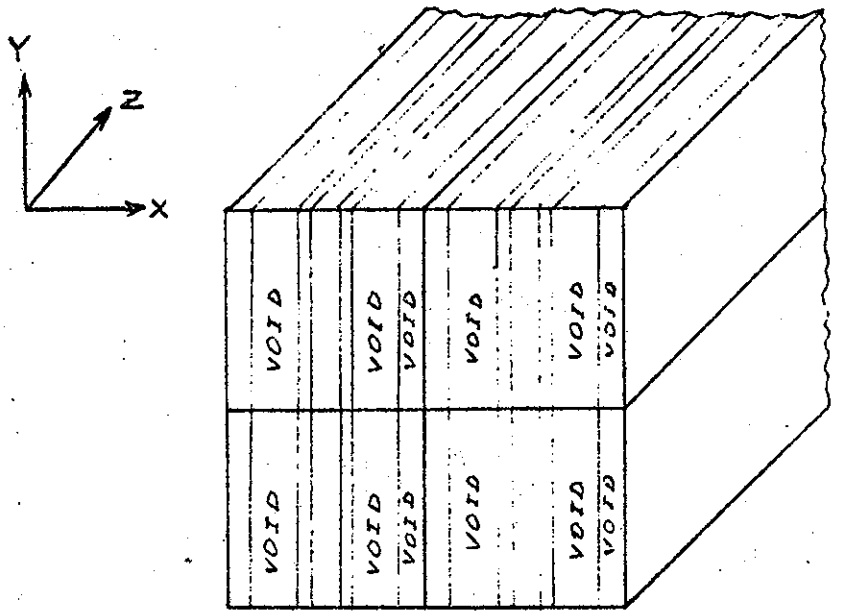

Normal drawer loading showing from drawers with all paltes positioned vertically. Direct streaming channels exist in the Y and Z directions.

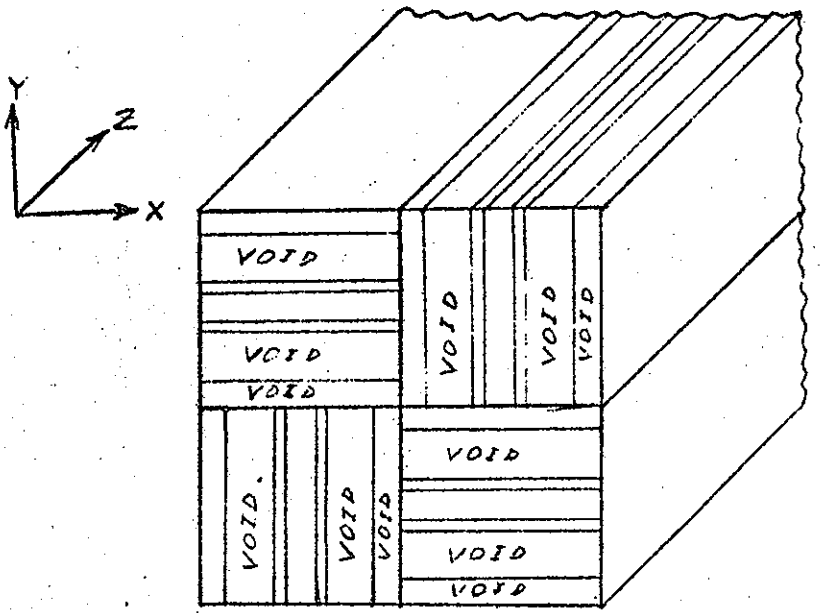

Checkerboard loading showing from drawers with plates in alternate drawers loading horizontally. Direct streaming channels now exist only in the Z direction.

Fig. 10. Illustration of the checkerboard loading concept. The actual unit cell compositions in the drawers are shown in Fig. 2.

Case 1: Plate Alignment is $\perp$ to leakage.

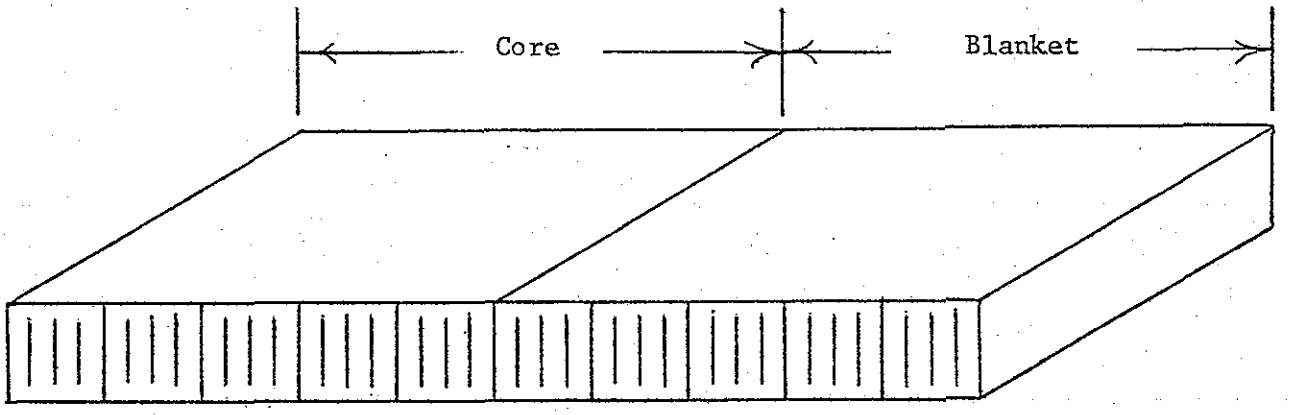

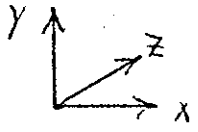

All exterior surfaces except $X = X_{max}$ have reflective boundary conditions. A vacuum boundary condition is used at $X = X_{max}$.

Case 2: Plate Alignment is $||$ to leakage.

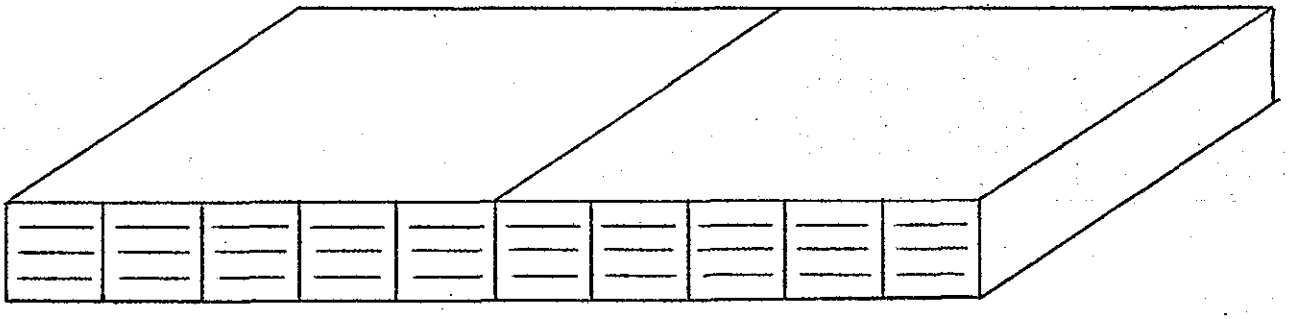

Fig. 11. Finite Medium Streaming Model Problem.